Production efficiency of excited atoms in PDP cells with grooved dielectric structures studied by laser absorption spectroscopy

AUTHOR(S):

Oh, JS; Tachibana, K; Hatanaka, H; Kim, YM; Son, SH; Jang, SH

CITATION:

Oh, JS ...[et al]. Production efficiency of excited atoms in PDP cells with grooved dielectric structures studied by laser absorption spectroscopy. IEEE TRANSACTIONS ON PLASMA SCIENCE 2006, 34(2): 376-384

ISSUE DATE:

2006-04

URL:

http://hdl.handle.net/2433/50087

Production Efficiency of Excited Atoms in PDP Cells With Grooved Dielectric Structures Studied by Laser Absorption Spectroscopy

Jun-Seok Oh, Kunihide Tachibana, *Member, IEEE*, Hidekazu Hatanaka, Young-Mo Kim, Seung-Hyun Son, and Sang-Hun Jang

***Abstract*—Performances of microplasmas in unit discharge cells with grooved structures in the dielectric layer covering the coplanar electrodes were investigated in alternating current (ac)-type plasma display panels filled with Ne–Xe(10%) mixture at 450 torr. The diagnostics are based on a microscopic laser-absorption spectroscopy technique for the spatiotemporally resolved measurements of absolute densities of $Xe^*(1s_5, 1s_4)$ atoms, from which the production rate and the efficiency of the vacuum ultraviolet photons were estimated. These results were compared with previously reported data obtained in conventional phosphor coated panels with the same structures for the dependences on the applied sustain voltages. As the result, the following conclusions were ascertained. The grooved structure does not help to improve the luminous efficiency but it helps to lower the firing and sustaining voltages by about 20 V if the electrode gap is kept constant. Therefore, it provides additional possibilities for the selection of other operating conditions such as the gas composition and pressure for the improvements of the luminance and the luminous efficiency.**

***Index Terms*—Excited atom density, grooved cell structure, luminous efficiency, plasma display panel.**

I. Introduction

IMPROVEMENT of luminous efficiency is the most important problem for the current plasma display panels (PDPs) to overcome the competition with other large-area flat panel displays such as liquid crystal displays [1]. Optimization of the structural issue for a unit discharge cell is the primarily important key toward the improvement in addition to the gas compositional issue. In a typical PDP cell, a three-electrode structure is commonly employed; a pair of coplanar sustain-electrodes are mounted on the front glass plate, which is covered successively with a thick dielectric film and a thin MgO film, and a data (or address) electrode is arranged on the back glass plate together with barrier ribs and a phosphor coated layer [1].

Manuscript received May 31, 2005; revised October 3, 2005. This work was supported in part by the SAIT Global Partner Project from Samsung Advanced Institute of Technology and in part by the Grants-in-Aid for Scientific Research on the Priority Area of Microplasmas from the Japanese Ministry of Education, Culture, Sports, Science and Technology.

J.-S. Oh and K. Tachibana are with the Department of Electronics Science and Engineering, Kyoto University, Kyoto 615-8501, Japan (e-mail: tatibana@kuee.kyoto-u.ac.jp).

H. Hatanaka, Y.-M. Kim, S.-H. Son, and S.-H. Jang are with the Materials Laboratory, Samsung Advanced Institute of Technology, Gyeonggi 449-712, Korea.

Digital Object Identifier 10.1109/TPS.2006.872431

For the improvement of the luminous efficiency from the structural issue, several approaches has been tried up to now. For instances, structures with T-shaped sustain electrodes [2], with the longer electrode gap [3], with a third auxiliary electrode [4], and with meander ribs [5] as well as new types of cell arrangements such as a delta array [6] and a new design with horizontal counter electrode structure [7]. Recently, a sophisticated design with a groove in the dielectric layer between the sustain electrodes has been studied [8]–[10]. The principal aim of this structure is to make the electric field concentrate at the ridges of the groove, and expect to lower the operating voltages and/or increase the production efficiency of excited atoms. Actually, it was reported that the discharge characteristics in the firing and the sustain voltages, and the discharge time lag (or response time) were improved by about 15%, 8%, and 8%, respectively, using two different types of grooves: a stripe groove and a box hollow groove [9]. Improvements of the luminance and the luminous efficiency were also ascertained in these cell structures with monochrome green phosphors [10]. However, in order to understand the mechanisms it is necessary to estimate the microplasma characteristics in a unit cell by making spatiotemporally resolved measurements of vacuum ultraviolet (VUV) emitting precursors for the phosphor excitation.

In this paper, we estimate the production efficiency of the total excited $Xe^*(1s_4, 1s_5)$ atoms in unit discharge cells with the same grooved structures as the previous ones in a comparison with normal cells with short and long electrode gaps. The measurements are performed by using our developed microscopic laser absorption spectroscopy (μLAS) technique [11]–[13]. Since those excited atoms are leading to the VUV emissions for the phosphor excitation, the luminance and the luminous efficiency can be discussed from the experimental results.

II. Experimental

A. Test Panels

We prepared four different types of panels of a 6-in diagonal size, which contain Ne–Xe(10%) at the same total pressure of 450 torr. The cell structures with grooves are shown schematically in Fig. 1(a) and (b) as Case 1 and Case 2. Case 1 had a stripe groove of 65 μm wide in the dielectric layer at the center of the electrode gap of 140 μm and Case 2 had a box hollow groove of 65 μm wide and 200 μm in length. Since the ridges are tapered,

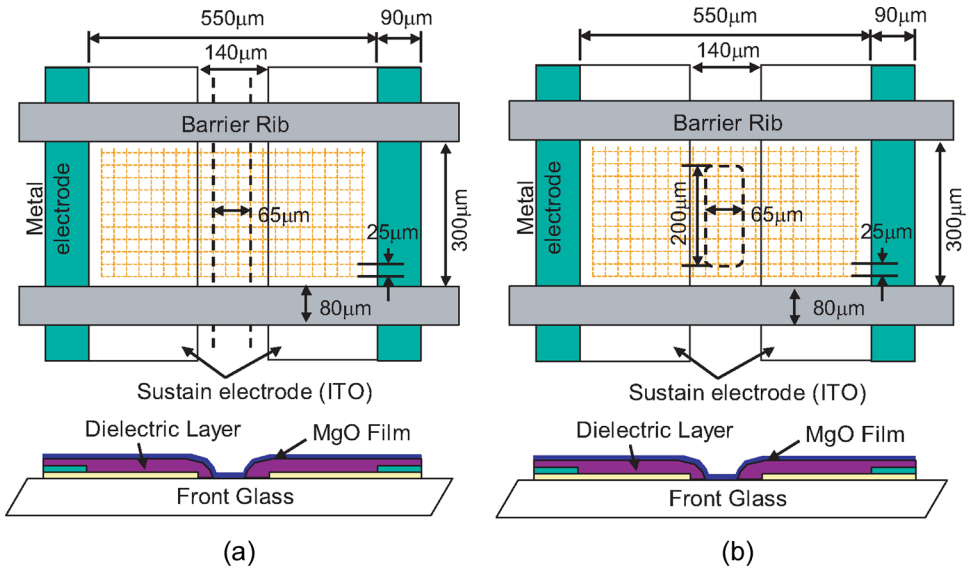

Fig. 1. Structures of unit discharge cells with (a) stripe shaped groove (Case 1) and (b) hollow shaped groove (Case 2) in between the sustain electrodes separated by 140 μm. Mapping points for the μLAS measurement are shown by grid points.

the sizes of the grooves given above are for those at the bottom. The other two panels had normal structures without grooves but the electrode gaps were 140 and 80 μm in Case 3 and Case 4, respectively. In each case, the thickness of the dielectric layer was about 35 μm, which was covered by an MgO film of about 0.5 μm to protect the dielectric surface from sputtering and to provide larger secondary electron emission under ion impacts [14]. The front glass plate was separated from the back one by 150 μm with barrier ribs. As opposed to a conventional cell structure, no address electrode and phosphor layer were deposited to allow the optical access by the probing laser beam. The operating pulses for the sustaining discharge were prepared by an arbitrary waveform generator combined with high speed voltage amplifiers, of which the pulse width, frequency and the rise time were 8.4 μs, 30 kHz, and 300 ns, respectively.

B. Experimental Setup and Procedure

The experimental setup of μLAS is the same as that described previously [11]–[13]. In short, the wavelength of a diode laser was tuned to the 823.1 nm $(1s_5 \rightarrow 2p_6)$ transition for the measurement of $Xe^*(1s_5)$ metastable atoms and the 828.0 nm $(1s_4 \rightarrow 2p_5)$ transition for $Xe^*(1s_4)$ resonance atoms. The laser beam was led through a test panel mounted on a movable stage of an optical microscope and the transmitted laser intensity was detected by a photomultiplier through a wavelength filtering monochromator. The typical beam diameter was about 15 μm at the center of the gas gap in a discharge cell. The measurement was performed at 21 $\times$ 11 points for the panels of Case 1 to Case 3 and 19 $\times$ 11 points for Case 4 panel in the horizontal plane of a discharge cell shown as mesh points in Fig 1. In the measurement, we experienced a difficulty in detecting the transmitted laser beam in the area near the edge of the groove, because the laser beam was refracted due to the gradual change in the thickness of the dielectric layer. We tried to adjust the position of the detection system to catch the deflected beam except positions in the quite vicinity of the edge where the beam diverged severely.

For the spatiotemporal behaviors of excited Xe atoms in the 2p levels, from which the 1s levels are partially populated by radiative cascades with the near infrared (NIR) emissions at around 800 nm, we used an intensified charge coupled device (ICCD) camera equipped with a bandpass filter centered at 820 nm. The gate width was set at 10 ns and the total exposure time was 3 seconds with a fixed gain throughout the present experiments. The waveform of the discharge current in a line containing 286 cells was measured by a digital oscilloscope using a differential probe across a series resistor of 425 Ω.

C. Derivation of Xe^* Production Efficiency

The luminous efficiency of a PDP is usually given by the ratio of the luminance of visible photons to the electric input power in units of lm/W. It contains several elemental factors: 1) the production efficiency of excited $Xe^*(1s_5, 1s_4)$ atoms; 2) the conversion efficiency of these atoms to the VUV photons via collisional and radiative processes; 3) the production efficiency of visible photons by phosphors; and 4) the geometrical factor for taking out the visible emission. In this paper, we are going to derive the factors 1) and 2) in order to investigate the differences between the cell structures in spatiotemporally resolved measurements. If the losses of $Xe^*(1s_5, 1s_4)$ atoms due to the diffusion, the stepwise ionization etc. can be neglected, most of the produced excited atoms are converted into VUV photons via the resonance radiation with an effective transition probability of imprisoned radiation for $Xe^*(1s_4)$ atoms and via Xe_2^* states followed by the excimer band emission for $Xe^*(1s_5)$ atoms and partially for $Xe^*(1s_4)$ atoms.

The measured density, however, does not give directly the production efficiency since the apparent density is the consequence of the balance between the production and the decay rates. Therefore, we can only derive the combined result of the two factors 1) and 2) for the production efficiency of VUV photons η [15]. The rate equation for the excited Xe atoms $n^*(r,t)$ depending on space r and time t can be written as

$$\frac{dn^*(r,t)}{dt} = g(r,t)N_0 - n^*(r,t)\gamma \qquad (1)$$

where $g(r,t)$ is the production rate, N_0 is the density of Xe atoms in the ground state, and γ is the decay rate of the excited atoms. The temporal integration of (1) over a halfcycle, where one of the sustain electrode is working as the anode and the other as the cathode, the left side term varnishes. Then, η is given by further integrating it over the whole space of a unit cell V and by dividing the result with the input power $P_{\rm in}$ as

$$\begin{aligned}\eta &\equiv \frac{1}{P_{\rm in}} \int_0^{\frac{T}{2}} \int_V g(r,t) N_0 dr dt \\ &= \frac{\gamma L}{P_{\rm in}} \int_0^{\frac{T}{2}} \int_S \bar{n}^*(x,y,t) dx dy dt \\ &= \frac{\gamma}{P_{\rm in}} \int_0^{\frac{T}{2}} N^*(t) dt \equiv \frac{\Gamma}{P_{\rm in}} \end{aligned} \tag{2}$$

where is the average density of excited atoms along the line of sight (equal to the cell thickness L) and $N^*(t)$ is the spatially integrated total number of excited atoms in a whole cell volume. Γ defined in the equation is the quantity which gives the total number of events for the production of excited atoms in a cell within a half cycle. Then, the overall VUV production efficiency is given by the sum of the contributions from $\mathrm{Xe}^*(1\mathrm{s}_5)$ atoms and $\mathrm{Xe}^*(1\mathrm{s}_4)$ atoms as

$$\begin{aligned}\eta &= \eta_m + \eta_r = \frac{1}{P_{\rm in}} \int_0^{\frac{T}{2}} (\gamma_m N_m^*(t) dt + \gamma_r N_r^*(t) dt) \\ &= \frac{(\Gamma_m + \Gamma_r)}{P_{\rm in}} \end{aligned} \tag{3}$$

where the suffixes m and r denote the quantities related to the metastable and resonance atoms.

III. Results

A. Spatiotemporal Behaviors of Excited Atoms

The spatiotemporal behaviors of the NIR image taken by the ICCD camera in a time sequence over a halfcycle in two test panels with grooves (Case 1 and Case 2) are shown in Fig. 2(a). Here, the left side electrode is working as the anode with the applied sustain pulse voltage V_s of 240 V and the right side is grounded as the cathode. It is seen that in both cases the discharge starts from the inner edge of the anode and soon after sharp and bright peaks appear at the ridge of the groove on the anode side. In Case 2, the bright spots tend to be more localized at the corner edge of the hollow ridge and bowed striations expand toward the outer end of the electrode. On the cathode side, a broad peak appears, expanding toward the outer end. It is seen that the emission image runs out to the region between the adjacent cells more noticeably in Case 1 because the groove makes open spaces beneath the barrier ribs. This may cause a problem of crosstalk between adjacent cells in the realistic operation of a PDP. Fig. 2(b) shows the corresponding images taken in Case 3 and Case 4 panels. In Case 3 with the wider electrode gap, the anode peak constrict to the center of the inner electrode edge, while it lengthened along the edge at the shorter gap in Case 4.

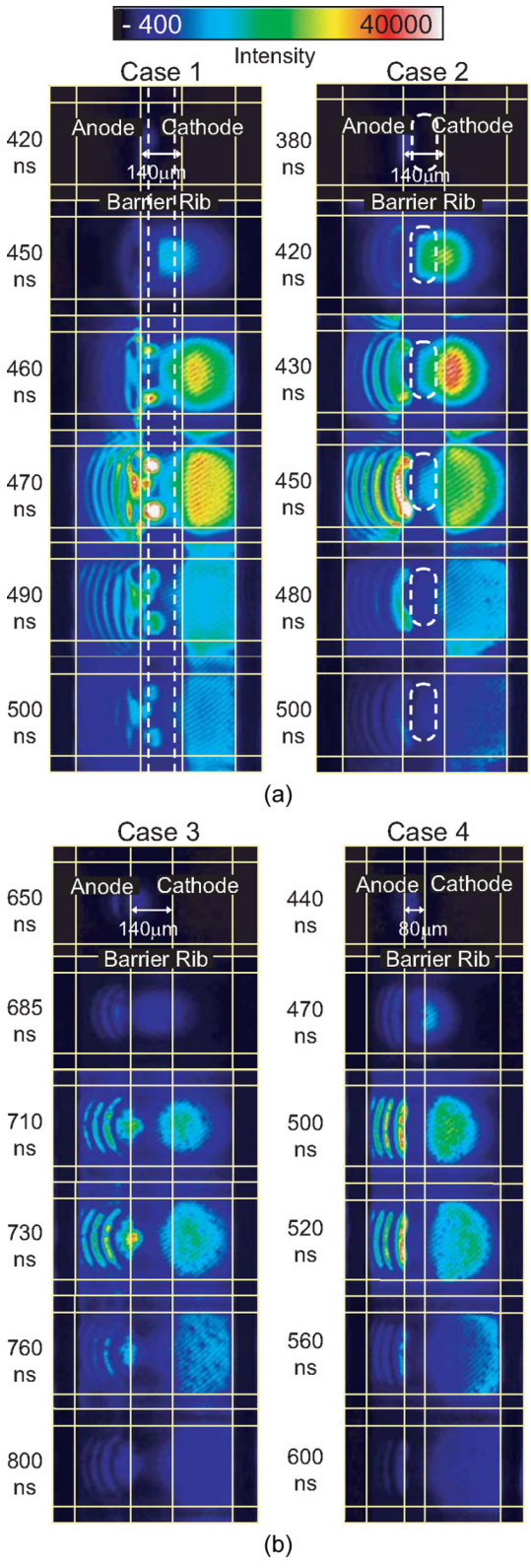

Fig. 2. Spatiotemporal image of the near IR emission measured (a) in stripe groove cell (Case 1) and hollow groove cell (Case 2), and (b) in normal cells without grooved structure with the different electrode gaps of 140 μm (Case 3) and 80 μm (Case 4) operated at a sustain voltage $V_s = 240$ V.

The spatiotemporal behaviors of the densities of $\mathrm{Xe}^*(1\mathrm{s}_5)$ atoms measured by μLAS are shown in Fig. 3(a) and (b) for all

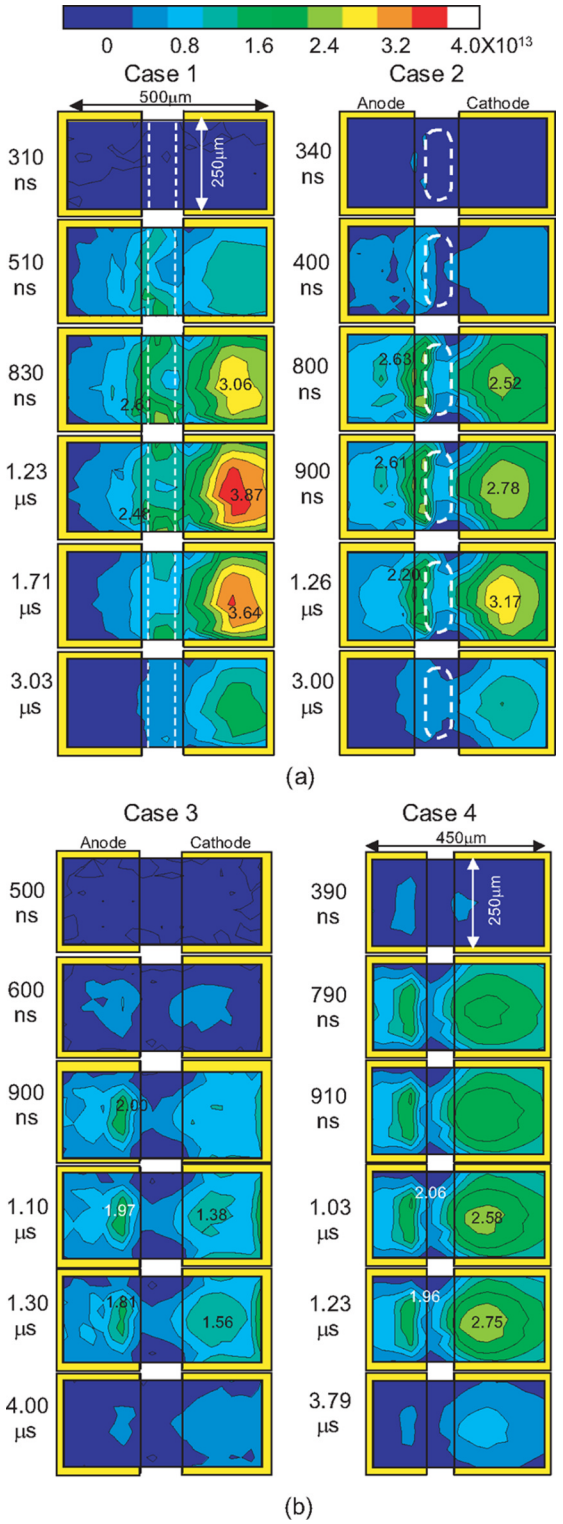

Fig. 3. Spatiotemporal behavior of $\mathrm{Xe}^*(1s_5)$ atom density (in units of 10^{13} cm^{-3}) measured (a) in stripe groove cell (Case 1) and hollow groove cell (Case 2), and (b) in normal cells without grooved structure with the different electrode gaps (Cases 3 and 4) operated at the sustain voltages $V_s = 230$ V for Case 1 and $V_s = 240$ V for Case 2 to 4.

four cases with the same experimental conditions as in Fig. 2. The characteristic features are similar to those of the NIR emission images except the much longer decay of the metastable atoms consistently with the previous observations [11]–[13]. In Case 1, doubly separated peaks are observed in the grooved area starting from the edge, while in Case 2 the sharper peaks appear at the outer edge of the hollow ridge. In both cases, a broad peak appears on the cathode side. The maximum density in these results ranges around $2 \sim 3 \times 10^{13}$ cm^{-3}. In the anode region, where the fine striated pattern is seen in the NIR image, but the metastable atom density is not high enough to recognize the structure. In Cases 3 and 4 without grooves, the characteristics of the density patterns are also similar to the NIR emission images shown in Fig. 2(b).

The corresponding results for the densities of $\mathrm{Xe}^*(1s_4)$ atoms are shown in Fig. 4(a) and (b). Basically, these are similar to the data of $\mathrm{Xe}^*(1s_5)$ atoms except a relatively short decay of the density (see below for the arguments on the decay constants). The double peaks at the anode side appear, of which the mutual distance is wider in the stripe groove structure (Case 1) than that in the hollow groove structure (Case 2). In both cases, the distance tends to increase with the increase in the applied sustain voltage. There appears also a broad peak on the cathode side. The maximum density in these data ranges around $0.8 \sim 1.2 \times 10^{13}$ cm^{-3}, which is smaller than the corresponding value of metastable atoms shown above.

B. Total Number of Excited $Xe^*(1s_4, 1s_5)$ Atoms

Here, we consider the temporal behaviors of the total number of metastable $(1s_5)$ atoms $N_m^*(t)$ and that of resonance $(1s_4)$ atoms $N_r^*(t)$ in a unit discharge cell. As defined in (2), these are obtained by integrating the density $n^*(r,t)$ over the whole cell area and multiplying the cell thickness L at each time step. The logarithmic plots of $N_m^*(t)$ measured in the grooved panels, Case 1 and Case 2, are shown in Fig. 5(a) and (b), respectively. Measurements were performed at several values of the sustain voltage V_s as given in the insets. The peak value of $N_m^*(t)$ ranges on the order of 10^8 atoms per cell and tends to increase with V_s. Similar plots have also been obtained for other panels, Cases 3 and 4, although those are not shown here. The peak values in these normal panels are slightly smaller than those in the grooved panels.

For the estimation of the quantity Γ_m defined in (3), we need to estimate for the decay rate γ_m of metastable atoms. This can be done from the logarithmic plots of $N_m^*(t)$, as shown in Fig. 5. The obtained values of γ_m are around 2.0 μs for all cases except Case 1 in which the values are relatively smaller. Looking at the raw data for Case 1 shown in Fig. 5(a) carefully, it is noticed that the decay is not singly exponential. The reason may be attributed to the additional diffusion loss to adjacent cells through the opening under the grooves, since the effect is larger at the early stage when the larger density of excited atoms locates near the barrier ribs.

The corresponding results of $N_r^*(t)$ for the resonance atoms are shown in Fig. 6(a) and (b), respectively, for Case 1 and Case 2. The peak values of $N_r^*(t)$ are $1 \sim 2 \times 10^8$ atoms per cell, which is smaller than those of metastable atoms by about three times. Values of the decay rate γ_r derived from the data in the figures are around 0.7 μs. Upon these preparations, we can now derive the quantities Γ_m and Γ_r for the metastable and resonance atoms defined in (3), of which the results are shown in Fig. 7(a) and (b), respectively. It is seen from the figures that the values of Γ_m are larger than those of Γ_r by about two times.

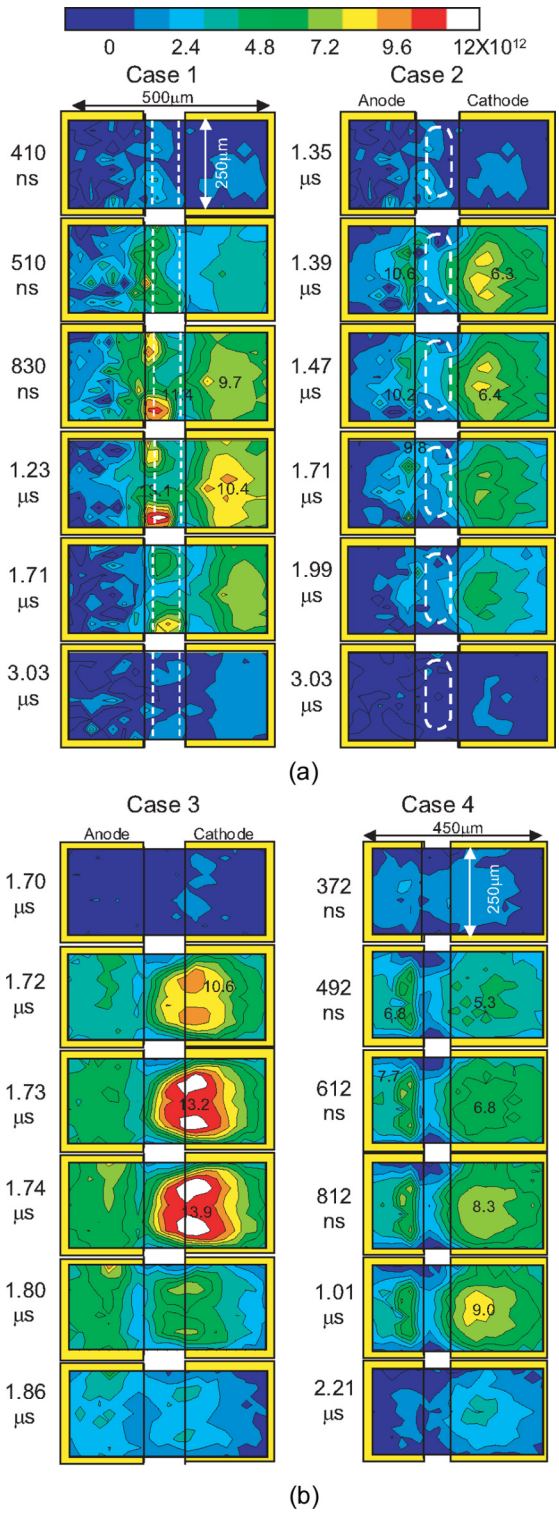

Fig. 4. Spatiotemporal behavior of $\mathrm{Xe}^*(1s_4)$ atom density (in units of 10^{12} cm^{-3}) measured (a) in stripe groove cell (Case 1) and hollow groove cell (Case 2), and (b) in normal cells without grooved structure with the different electrode gaps (Cases 3 and 4) operated at the same condition given in Fig. 3.

This result is consistent with our previously reported data at the same Xe concentration [15]. Similarly, the consistency in the results of the decay rates, γ_m and γ_r is also ascertained. (See the arguments given there for the comparison of the experimental values with the estimated values from the reported data such as the rate constants for the three-body collisions and the escape factor of the imprisoned resonance radiation.)

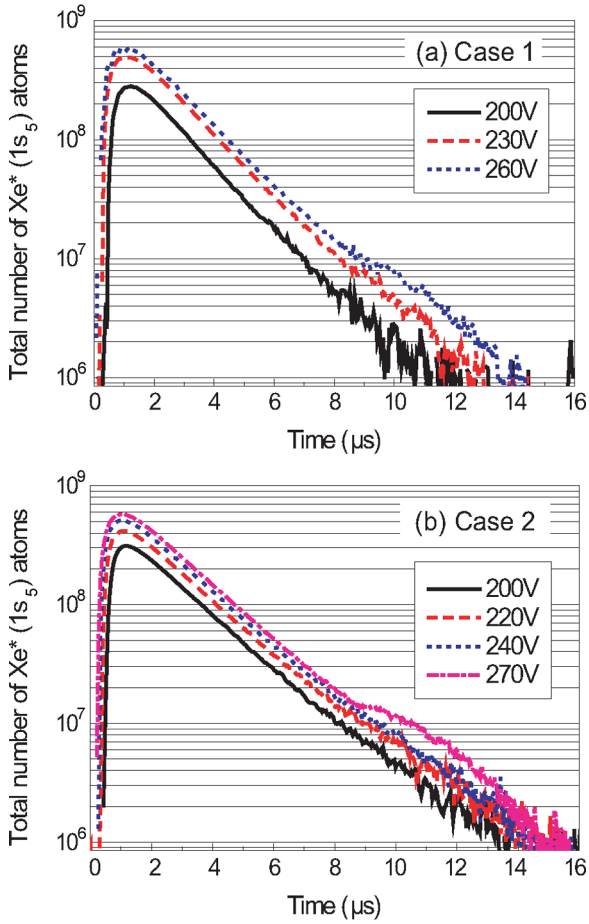

Fig. 5. Temporal behavior of the total number of $\mathrm{Xe}^*(1s_5)$ atoms in a cell measured at several values of V_s in stripe groove cell (Case 1) and hollow groove cell (Case 2).

These results suggest that the contribution of the atomic line at 147 nm from resonance atoms to the VUV emissions is about a half of that of the excimer band at 173 nm mainly from metastable atoms.

C. Input Power

The input power P_{in} into a unit discharge cell was derived by integrating the discharge current I multiplied by the sustain voltage V_s. Fig. 8 shows the obtained values of P_{in} in the four panels as a function of V_s. In all cases, P_{in} increases almost linearly with V_s, but it is relatively larger in the grooved panels (Cases 1 and 2) than the normal panels (Cases 3 and 4).

To investigate the reason, the measured current waveforms are shown in Fig. 9 for all the cases. In every case, the waveform becomes sharper with a larger peak value as V_s increases. However, the discharge delay time (or response time) is relatively shorter in the grooved panels than in the normal panels with the same electrode gap (Case 3). Therefore, it is necessary to make the gap shorter to decrease the response time, as seen in Case 4. It is noted here that the current waveform in Case 1 is doubly peaked. That is comparable with Case 2. See the spatiotemporal behaviors of IR emission in Fig. 2(a) and $\mathrm{Xe}^*(1s_4)$ density in Fig. 4(a). The first peak corresponds to the appearance of emission peaks along the ridge and the second peak does to the striated peaks on the anode side in Case 1. The discharge at

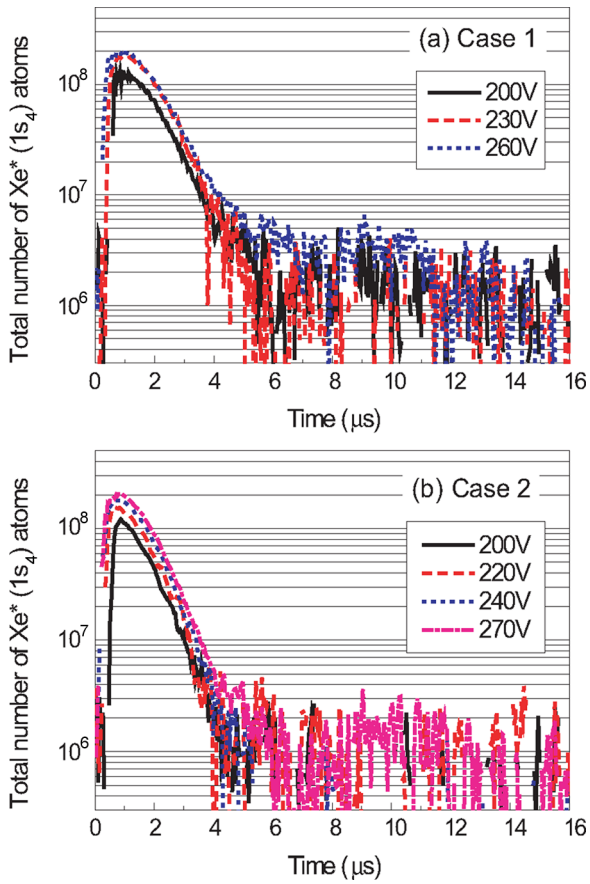

Fig. 6. Temporal behavior of the total number of $\mathrm{Xe}^*(1s_4)$ atoms in a cell measured at several values of V_s in stripe groove cell (Case 1) and hollow groove cell (Case 2).

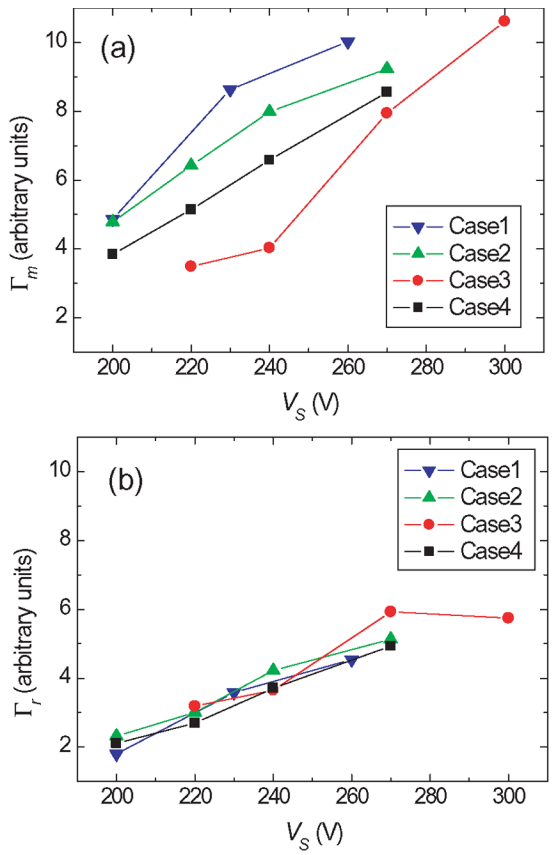

Fig. 7. Production rate of (a) $\mathrm{Xe}^*(1s_5)$ atoms Γ_m and (b) $\mathrm{Xe}^*(1s_4)$ atoms Γ_r measured in four test panels (Cases 1 to 4) as a function of V_s.

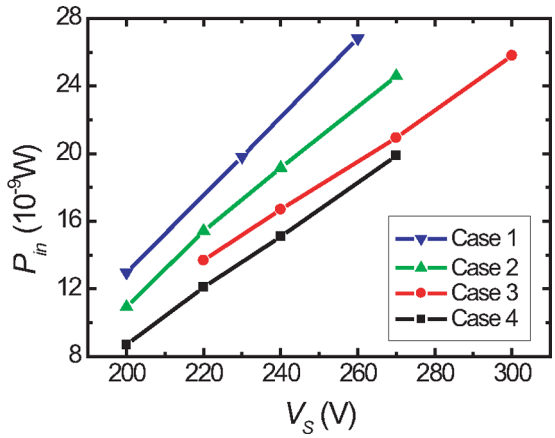

Fig. 8. Input power in a unit cell estimated for four test panels as a function of V_s.

the ridge occurs near the ribs with separated peaks, and it might trigger the main discharge in the central part of the anode edge with a certain time delay.

On the other hand, only a single sharp current peak appears in Case 2, even with a grooved structure. This may be due to the fact that both corners of the hollow groove are closer to the center of the electrode edge, and those ridged parts form a unified bowed shape of the strongest electric field as can be seen in the behavior of the emission shape on the anode side in Fig. 2(a) appearing as a single bowed structure.

D. Production Efficiency

The final results for the production efficiency of VUV photons η_T obtained by adding the contributions from the metastable and resonance atoms are shown in Fig. 10. It is seen that the results are more favorable for the grooved structures (Cases 1 and 2) than the normal structure (Case 3) at lower values of the sustain voltage V_s if the electrode gap is fixed at the same value of 140 μm. However, when the gap is shortened to 80 μm, there are no apparent merits of these sophisticated structures as compared to the normal structure (Case 4). Further arguments will be done below.

IV. Discussion

In this section, we discuss our results in a comparison with the previous results by Son *et al.* [8] and Nam *et al.* [9], [10]. Actually, we employed the same structures as theirs, but the difference in practice is that the phosphor layers are not present in our panels. That might be the reason for the relatively higher operation voltages in our experiments than the previous values by about 20 V both in the grooved structures and the normal structures.

The luminance can be estimated in a relative scale from the data of Γ_m and Γ_r given in Fig. 7, although the absolute values cannot be given in our measurements. When we compare the results with the data shown in [10, Fig. 6], the linearly increasing

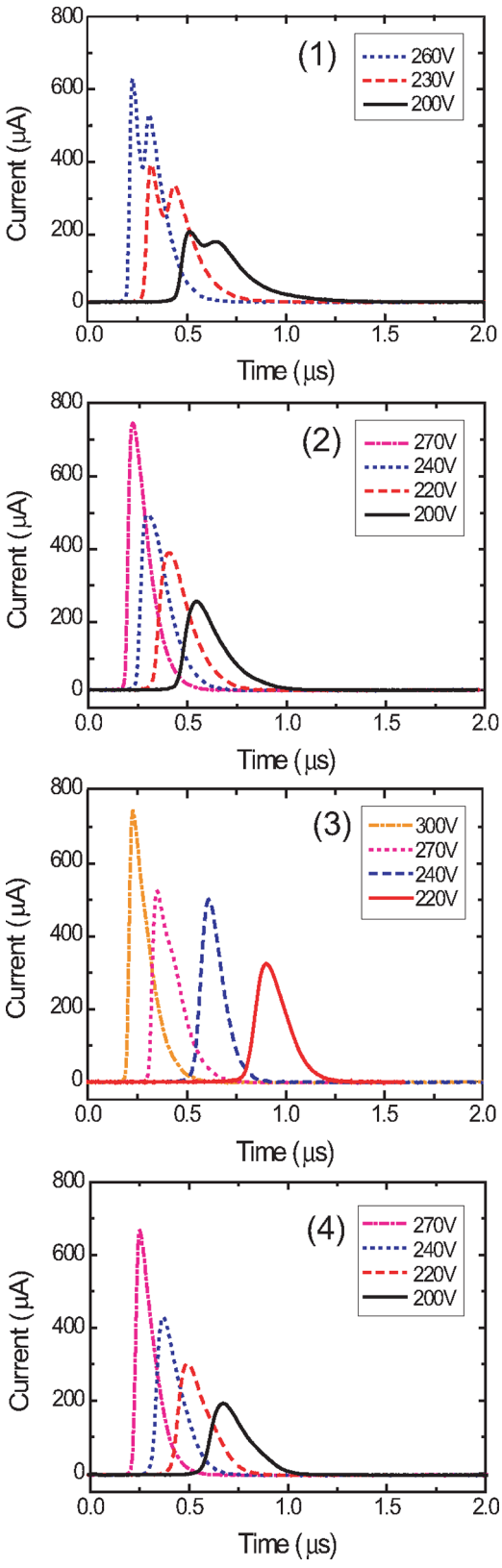

Fig. 9. Waveforms of the discharge current in a unit cell of four test panels measured at several values of V_s.

tendency of the luminance with the sustain voltage V_s is consistent with each other except that a slightly saturating tendency can be seen in the previous data at higher V_s.

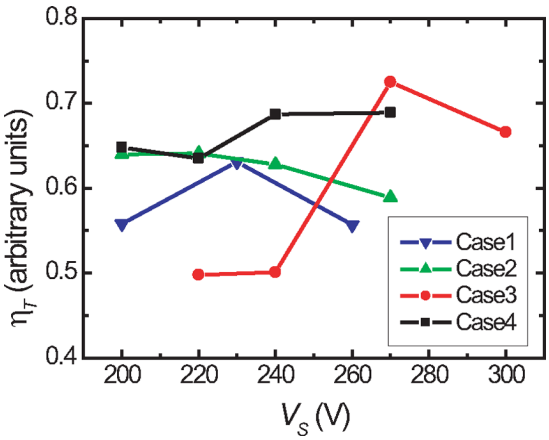

Fig. 10. Overall production efficiency of VUV photons from $\mathrm{Xe}^*(1s_5, 1s_4)$ atoms estimated in four test panels as a function of V_s.

In the comparison of the luminous efficiency of the present experiments given in Fig. 10 with the previous data shown in [10, Fig. 8], there appear large differences. In the previous data the efficiency decreases monotonously with V_s in all cases irrespective of the structures. In contrast, in the present experiments the efficiency roughly tends to decrease in the grooved structure panels (Cases 1 and 2), but keeps steady or rather increases with V_s in a normal structure panel with a shorter gap (Case 4). The data points of a longer gap normal panel (Case 3) behave more differently. However, the two data points at the lower values of V_s for Case 3 might be too low due to the fact that the discharge is not well developed, as can be seen in Fig. 2(b), where a concentrated sharp peak appears at the anode edge and the area of the cathode peak does not fully developed between the barrier ribs. As V_s is increased, the anode peak becomes longer, as seen in Case 4 in the same figure corresponding to a shape of a well developed discharge. In that situation, the generally observed tendency of higher efficiency with longer gap can be seen above $V_s = 270$ V in our cases.

In order to derive the luminous efficiency, however, we have to divide the production efficiency by the data of power P_{in}, as shown in Fig. 8. Therefore, the difference in the general tendency of our data from those of [10] might also be attributed to the difference in the estimated values of P_{in}. Since no direct data of P_{in} are given there, we cannot discuss further the different behaviors.

In any case, the following conclusions on the luminous efficiency are commonly drawn to our data and the previous data. First, the efficiency cannot be improved by the grooved structures itself. Second, the operating voltages can be lowered by about 20 V by using grooved structures if the electrode gap is the same. To say conversely, we can adopt a longer gap length with the grooved structure without increasing the operating voltages. The lowering of the voltages is a favorable result for making possible choices of other operation conditions, say increasing the Xe concentration or the total pressure.

V. Conclusion

For improvements of the luminance and the luminous efficiency, the performances of the new cell structures with

grooves in the dielectric layer between the sustain electrodes were investigated. Spatiotemporal behaviors of the excited $Xe^*(1s_4, 1s_5)$ atoms were measured by the μLAS method. With these results, we tried to estimate the production rate of these excited atoms and converted it into the relative production efficiency of VUV photons normalized by the input power. As the result, it is proved that the grooved structure does not help to improve the luminous efficiency but it helps to lower the firing and sustaining voltages by about 20 V if the electrode gap is kept constant. Therefore, it produces additional possibilities for the selection of other operating conditions such as the gas composition and pressure for the improvements of the luminance and the luminous efficiency.

REFERENCES

[1] J. P. Boeuf, "Plasma display panels: Physics, recent developments and key issues," *J. Phys. D, Appl. Phys.*, vol. 36, pp. R53–R79, 2003.

[2] C. Koshio, H. Taniguchi, K. Amemiya, N. Saegusa, T. Komaki, and Y. Sato, "New high luminance 50-inch AC PDP's with an improved panel structure using 'T'-shaped electrodes and 'Waffle'-structured ribs," in *Proc. 8th Int. Display Workshops*, Nagoya, Japan, 2001, pp. 781–784.

[3] A. Lacoste, L. Tessier, D. Gagnot, and H. Doyeux, "Long gap discharge with triggering controlled by short pulses for AC PDPs," in *Proc. 10th Int. Display Workshops*, Fukuoka, Japan, 2003, pp. 1013–1016.

[4] Y. Shintani, J. C. Ahn, K. Tachibana, N. Kosugi, and T. Sakai, "Diagnostics and control of three-dimensional behaviors of microdischarge in a unit cell of an ac-type plasma display panel," *J. Phys. D, Appl. Phys.*, vol. 36, pp. 2928–2939, 2003.

[5] O. Toyoda, T. Kosaka, F. Namiki, A. Tokai, H. Inoue, and K. Betsui, "A high performance delta arrangement cell PDP with meander barrier ribs," in *Proc. 6th Int. Display Workshops*, Sendai, Japan, 1999, pp. 599–602.

[6] S. Harada, S. Yura, K. Morikawa, and K. Sano, "New delta arranged cell configuration of ac plasma display 'DIA-PDP' for high luminous efficiency and high resolution," *Electr. Commun. Jpn.*, pt. 2, vol. 87, pp. 9–17, 2004.

[7] K. Tachibana, S. Kawai, H. Asai, N. Kikuchi, and S. Sakamoto, "Characteristics of Ne-Xe microplasma in unit discharge cell of plasma display panel equipped with counter sustain electrodes and auxiliary electrodes," *J. Phys. D, Appl. Phys.*, vol. 38, pp. 1739–1749, 2005.

[8] S.-H. Son, Y.-S. Park, S.-C. Bae, and S.-Y. Choi, "Application of hollow channel between sustain electrodes to improve discharge characteristics in alternating current plasma display panels," *Appl. Phys. Lett.*, vol. 80, pp. 1719–1721, 2002.

[9] M.-H. Nam, J.-M. Kim, S.-Y. Choi, S.-H. Son, and Y.-M. Kim, "Characteristics of plasma display panel with ridged dielectric and hollow gap between sustain electrodes," *J. Appl. Phys.*, vol. 96, pp. 993–996, 2004.

[10] M.-H. Nam, S.-Y. Choi, S.-H. Son, and Y.-M. Kim, "Discharge characteristics of plasma display panel with box-shaped apertures in transparent dielectric layer," *J. Appl. Phys.*, vol. 97, no. 073304, 2005.

[11] K. Tachibana, N. Kosugi, and T. Sakai, "Spatio-temporal measurement of excited $Xe(1s_4)$ atoms in a discharge cell of a plasma display panel by laser spectroscopic microscopy," *Appl. Phys. Lett.*, vol. 65, pp. 935–937, 1994.

[12] K. Tachibana, S. Feng, and T. Sakai, "Spatiotemporal behaviors of excited Xe atoms in unit discharge cell of ac-type plasma display panel studied by laser spectroscopic microscopy," *J. Appl. Phys.*, vol. 88, pp. 4967–4974, 2000.

[13] K. Tachibana, K. Mizokami, N. Kosugi, and T. Sakai, "Three-dimensional diagnostics of dynamic behaviors of excited atoms in microplasma for plasma display panels," *IEEE Trans. Plasma Sci.*, vol. 31, no. 1, pp. 68–73, Feb. 2003.

[14] H. Uchiike, K. Miura, N. Nakayama, T. Shinoda, and Y. Fukushima, "Secondary electron emission characteristics of dielectric materials in AC-operated plasma display panels," *IEEE Trans. Electron Devices*, vol. ED-23, no. 11, pp. 1211–1217, Nov. 1976.

[15] J.-S. Oh, K. Tachibana, H. Hatanaka, Y.-M. Kim, S.-H. Son, and S.-H. Jang, "Production efficiencies of $Kr^*(1s_5, 1s_4)$ atoms leading to vacuum-ultraviolet emissions in ac plasma display panels with Kr-Ne binary mixtures measured by laser-absorption spectroscopy," *J. Appl. Phys.*, vol. 98, no. 103302, 2005.

Jun-Seok Oh received the B.S. and M.S. degrees in Department of Electrophysics, Kwangwoon University, Seoul, Korea, in 2001 and 2003, respectively. When he was a M.S. student, his research focused on the MgO thin films for protecting of dielectric layer in AC-PDP. He is currently working toward the Ph.D. degree in the Department of Electronic Science and Engineering, Kyoto University, Kyoto, Japan.

His current research focuses on the high efficiency plasma display panels.

Kunihide Tachibana (M'02) received the B.S., M.S., and Ph.D. degrees from Kyoto University, Kyoto, Japan, in 1968, 1970, and 1973, respectively.

He joined the Department of Electronics, Kyoto Institute of Technology, in 1974 and became a Full Professor in 1988. He moved to the Department of Electronic Science and Engineering, Kyoto University in 1995 as a Full Professor. His research subjects include plasma diagnostics with lasers and other spectroscopic techniques in various kinds of plasmas for material processing, light sources, and display devices. His current research interest is shifting toward microplasmas and atmospheric pressure discharges.

Dr. Tachibana is a member of The Japan Society of Applied Physics, American Vacuum Society, etc., and is serving as the President of International Plasma Chemistry Society.

Hidekazu Hatanaka received the B.S., M.S., and Ph.D. degrees in electrical engineering from Keio University, Kanagawa, Japan, in 1988, 1990, and 1993, respectively.

In 1993, he was a Visiting Scientist of Keio University. From 1993 to 1995, he was a Postdoctoral Research Fellow in Los Alamos National Laboratory, Los Alamos, NM. From 1995 to 1999, he worked at NEC Corporation, Sagamihara, Japan, where he engaged in development of laser diode pumped solid-state lasers and wavelength conversion technology. Since 2000, he has been a member of technical staff with Samsung Advanced Institute of Technology, Gyeonggi, Korea. His current research activities are on plasma display.

Young-Mo Kim received his B.E and M.E. degrees in nuclear engineering from Seoul National University, Seoul, Korea, in 1991 and 1993, respectively, and the Ph.D. degree in mechanical engineering from RWTH, Aachen, Germany, in 1999.

From 1994 to 1999, he was a Guest Scientist at the Institute of Plasma Physics of Research Center, Juelich, Germany, working mainly on experimental plasma physics at a great fusion project (TEXTOR). Since 1999, He has been a member of researcher staff of Samsung Advanced Institute of Technology, Gyeonggi, Korea. His current research area is plasma display, especially development of highly efficient PDP with new gas discharges.

Seung-Hyun Son received the B.S., M.S., and Ph.D. degrees in electronic engineering from Kyungpook National University, Daegu, Korea, in 1996, 1998, and 2002, respectively.

Since 2002, he has been a member of researcher staff of Samsung Advanced Institute of Technology, Gyeonggi, Korea. His current research area is plasma display, especially display materials, display process.

Sang-Hoon Jang received the B.S. and M.S. degrees in electrical engineering and the Ph.D. degree in electronic engineering from Kyungpook National University, Daegu, Korea, in 1996, 1998, and 2002, respectively.

Since 2003, he has be a member of researcher staff of Samsung Advanced Institute of Technology, Gyeonggi, Korea. His current research area is plasma display, especially development.